

Light Emission From Hydrogenated and Unhydrogenated Si-Nanocrystal/Si Dioxide Composites Based on PECVD-Grown Si-Rich Si Oxide Films

David Comedi, Othman H. Y. Zalloum, Jacek Wojcik, and Peter Mascher

Abstract—Hydrogenated and unhydrogenated Si-nanocrystal/Si dioxide (Si-nc/SiO₂) composites were obtained from Si_yO_{1-y} ($y = 0.36, 0.42$) thin films deposited by plasma-enhanced chemical vapor deposition. The unhydrogenated composites were fabricated by promoting the Si precipitation through the thermal annealing of the films in the flowing pure Ar at temperatures up to 1100 °C. The hydrogenated composites were obtained from identical films by replacing the Ar with (Ar + 5% H₂) in the annealing step. The photoluminescence (PL) of the composites was studied as a function of the annealing temperature (T), annealing time, and pump laser power. The PL intensity increases with increasing annealing temperature and time; however, it increases faster and attains several hundreds percent larger values when the annealing is performed under (Ar + 5% H₂) as compared to the annealing under pure Ar. Fourier-transform infrared spectra show that H in these hydrogenated samples incorporates mainly as Si-H bonds. The dependence of the PL spectra on y , T , and laser power are consistent with the assumption that light emission in both the hydrogenated and unhydrogenated Si-nc/SiO₂ composites originates from the bandgap transitions involving the electron quantum confinement in the Si-ncs. The PL spectra from the hydrogenated films are skewed to the red as compared to those from the unhydrogenated ones. The bulk of the data indicates that H passivates the nonradiative recombination centers, most probably Si dangling bonds in disordered Si-nc/SiO₂ regions, thus increasing the number of Si-ncs that contribute to the PL and modifying the distribution of the emission wavelengths.

Index Terms—Nanotechnology, photoluminescence (PL), plasma chemical-vapor deposition (CVD), semiconductor films, silicon.

I. INTRODUCTION

THE fabrication of the light sources from Si has proven to be the major challenge in Si photonics [1]. This is mainly due to the poor emission efficiency of bulk Si, which, in turn, is a consequence of its indirect bandgap. The use of the conventional III-V material light emitters in Si-photonics integrated

Manuscript received October 31, 2005; revised September 21, 2006. This work was supported in part by Ontario Research and Development Challenge Fund (ORDCF) under the Ontario Photonics Consortium (OPC) and in part by the Ontario Centres of Excellence (OCE), Inc.

D. Comedi was with the Center for Emerging Device Technologies and the Department of Engineering Physics, McMaster University, Hamilton, ON L8S 4L7, Canada. He is now with CONICET and LAFISO, Departamento de Física, FACET, Universidad Nacional de Tucumán, Tucumán, Argentina (e-mail: dcomedi@herrera.unt.edu.ar).

O. H. Y. Zalloum, J. Wojcik, and P. Mascher are with the Centre for Emerging Device Technologies and the Department of Engineering Physics, McMaster University, Hamilton, ON L8S 4L7, Canada (e-mail: zalloum@mcmaster.ca; wojcikj@mcmaster.ca; mascher@mcmaster.ca).

Digital Object Identifier 10.1109/JSTQE.2006.885388

systems has so far circumvented this problem [2]. Such an approach, however, relinquishes the most important appeal of the Si-photonics technology, namely the use of fully CMOS compatible processes at every fabrication stage. Indeed, the development of a Si laser would allow economical and mass production of the monolithically integrated optoelectronic on-a-chip systems. It is in the recognition of this fact that much work on the Si light sources has been done in recent years [3]–[6]. Significant achievements have been obtained albeit the field is still far from having reached maturity.

A promising line of research concentrates on the luminescent Si nanostructures such as porous Si (PS) obtained by the anodic wet etching of Si wafers [7]. Pioneering efforts showed light emission in PS to be consistent with the quantum confinement (QC) effect in Si nanocrystals (Si-nc), which are known to be produced in the etching process [8]. The luminescence efficiency from PS, however, was shown to degrade with time as a result of the buildup of a native oxide at the Si-nc surfaces that replaces the Si-H bonds originally present in the as-etched material [9]. This triggered a considerable amount of research on several alternative methods to synthesize Si-ncs. An interesting technique, which is fully CMOS compatible, takes advantage of the well-known good passivation and stability of the Si/SiO₂ interface by dispersing the Si-ncs in an amorphous SiO₂ matrix [10], [11]. Such a Si-nc/SiO₂ composite can be easily obtained by promoting the decomposition of the substoichiometric Si oxides (Si_yO_{1-y}, where $y > 1/3$) into SiO₂ and elemental Si phases through thermal annealing above 900 °C. Metastable Si_yO_{1-y} films, in turn, can be obtained by the ion implantation [10] of Si into silica or by the vapor deposition methods [11], [12]. The phase separation process, the evolution of the amorphous Si oxide, the precipitation of Si, and the formation of Si-ncs have been studied in considerable detail [13]–[16]. The Si-nc mean size increases with increasing excess Si concentration, annealing temperature, or annealing duration. Efficient photoluminescence (PL) in the visible region has also been observed in these materials, which appears as Si-ncs are formed [15]–[18]. The dependence of the PL intensity and energy on the Si-nc mean size supports the hypothesis that as in PS, QC plays a major role in the emission process in these materials. However, studies have indicated that the details of the recombination mechanisms are strongly influenced by the electronic states in the Si-nc/SiO₂ interface region [19]–[21], which is not sharp in structure and composition. Si dangling

bonds (dbs) were found to be the major luminescence killers due to their large electron–hole capture cross section [22]. The passivation by H of these dbs was demonstrated; however, it has been argued that H could produce additional chemical changes at the Si-nc/SiO₂ interface [23], [24] or promote the formation of siloxene [25].

The effects of H on the PL from the Si-nc/SiO₂ composites have been studied mostly for materials obtained from the Si_yO_{1-y} films synthesized by the ion implantation [26]–[31]. In most cases, the incorporation of H was found to yield a significant increase of the PL intensity, which was ascribed to the passivation of the Si dbs. Few authors, however, reported on other effects induced by H, such as the spectral redistribution of the PL, and some possible explanations for this effect have been put forward [31].

In this paper, we compare the behavior of the PL intensity as a function of the annealing temperature, annealing time, and optical pumping power for the hydrogenated and unhydrogenated Si-nc/SiO₂ samples prepared from the Si_yO_{1-y} films deposited by electron cyclotron resonance plasma-enhanced chemical-vapor deposition (ECR-PECVD). The PL measurements are complemented by the Fourier-transform infrared (FTIR) spectroscopy and elastic recoil detection analysis (ERDA) to obtain information on the H incorporation.

II. EXPERIMENTAL DETAILS

The Si_yO_{1-y} films were deposited on the single-side polished c-Si(1 0 0) substrates held at 120 °C using an ECR-PECVD system described elsewhere [32]. For the FTIR study, some of the films were deposited on the double-side polished c-Si(1 0 0) substrates. The thickness of the films was around 2 μm and the *y* values were 0.36 and 0.42 [33]. The annealing of the films was performed in a quartz tube furnace under either Ar or (Ar + 5% H₂) atmospheres for time ranging from 30 min to 3 h and at temperatures up to 1100 °C. At the end of the annealing runs, the samples were slowly transferred to a lower temperature region in the furnace while keeping the same annealing atmosphere until they attained the room temperature. This cooling procedure took 15 min. The PL measurements were carried out at room temperature using the 325 nm line of a He–Cd laser and an Ocean Optics spectrometer with the maximum incident effective power of ~0.64 W/cm². All the PL spectra were corrected for the detection system response. The laser pump power dependence of the PL was determined by repeating the measurements with the incident laser power attenuated by the neutral density filters. The ERDA measurements were performed at the University of Western Ontario using a 1.6 MeV He⁺ beam. FTIR measurements were performed in the transmission mode between 4000 and 350 cm⁻¹.

III. RESULT

A. Dependence of the PL on the Annealing Parameters

Fig. 1(a) shows the typical PL spectra obtained for the Si_yO_{1-y} (*y* = 0.36) films annealed in (Ar + 5% H₂) at three different temperatures (*T*). Also shown is the spectrum from an

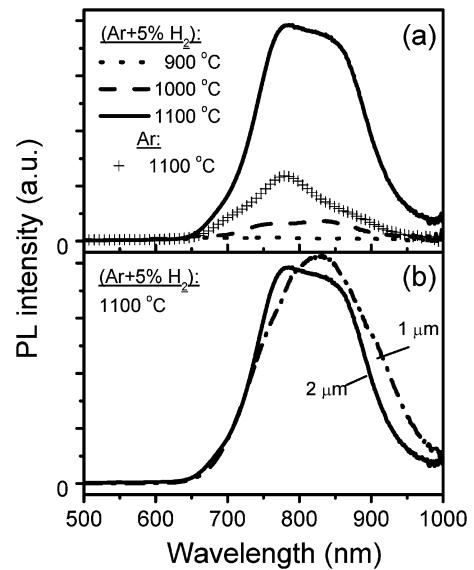


Fig. 1. (a) PL spectra as obtained for the Si_yO_{1-y} (*y* = 0.36) 2-μm thick films annealed in the flowing Ar at 1100 °C (+) and in the flowing (Ar + 5% H₂) at 900 °C (dotted line), 1000 °C (dashed line), and 1100 °C (solid lines). The annealing duration was 2 h. (b) The data corresponding to the sample annealed at 1100 °C in (Ar + 5% H₂) from (a) and compared with the similar data obtained for a thinner (1-μm thick) film that was annealed under identical conditions.

identical sample annealed in pure Ar at 1100 °C. The PL intensities from as-grown films or from films annealed at *T* ≤ 800 °C are within the noise level and are not shown in the figure. The weak modulation superimposed on the peaks shown in Fig. 1 is believed to be due to the multiple interference effects on the reflectivity [34]. This has been particularly confirmed for the sample annealed at 1100 °C in the (Ar + 5% H₂) data. The apparent “double-peak character” of this spectrum is an artifact due to a small valley that occurs on the top of the peak, which is probably just due to an interference dip that is particularly visible as it happens to be in a low-derivative region of the spectrum (i.e., at its maximum). To confirm this, we have repeated the annealing processes and measurements in a similar Si_yO_{1-y} sample with a different thickness (1 μm instead of 2 μm). The corresponding spectra for the 1100 °C annealing in (Ar + 5% H₂) are compared in Fig. 1(b). It can be noted that no “double peak structure” is apparent for the 1-μm thick sample, although the annealing parameters were kept identical to those used for the thicker film. The slight relative redshift of the peak with respect to that for the thicker film is probably due to a slightly different Si excess concentration achieved in this particular PECVD growth. Hence, throughout this paper, we refrain from making any strong argument based on the shapes of the PL peak, except for the well-documented fact that the PL peak widths are, in general, related to the relatively wide Si-nc size distributions achieved by the kind of fabrication technique used here [11].

Returning to Fig. 1(a), it can be seen that the annealing at *T* = 900 °C leads to a barely measurable PL intensity, which increases abruptly as *T* increases to 1000 °C and 1100 °C. This effect is accompanied by a slight redshift of the PL peak. Previous X-ray diffraction (XRD) studies in similar samples [14], [18]

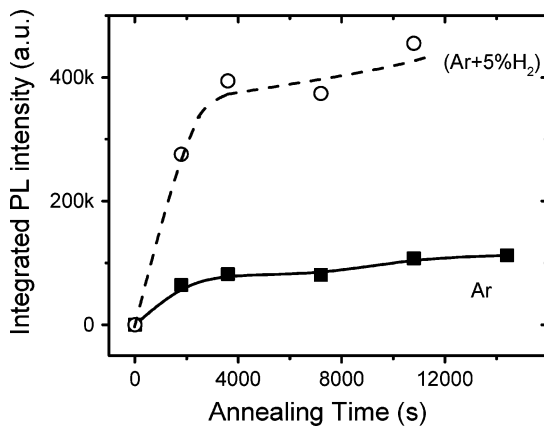


Fig. 2. Fully integrated PL intensity from the $\text{Si}_y\text{O}_{1-y}$ ($y = 0.36$) films annealed at 1100°C in the flowing ($\text{Ar} + 5\% \text{H}_2$) (circles) and Ar (squares), as a function of the annealing duration. The point at the origin corresponds to the unannealed (as-grown) sample. The lines are guides to the eye.

have shown that the phase separation and the Si-nc formation occurs in the same temperature range. Hence, the increase of the PL intensity can, possibly, be associated with the formation of an increasing number of Si-ncs. Furthermore, the mean Si-nc size has also been shown to be an increasing function of T , presumably due to the increase of the Si diffusivity in the Si oxide [14]. The slight redshift of the PL peak with the increasing T is consistent with the QC effect, which predicts a gradual decrease of the Si-nc bandgap toward the value in the bulk Si as the Si-nc mean size increases.

Fig. 2 shows the integrated PL intensity as a function of the annealing time at 1100°C for samples annealed in Ar and ($\text{Ar} + 5\% \text{H}_2$). It can be seen that in both the cases, PL rapidly increases from zero and tends to saturate for times above 4000 s. Hence, it seems that the main effect of adding 5% H_2 to the annealing gas is in increasing the total PL intensity by a factor of about 5, which depends weakly on the annealing time.

This weak time dependence is reasonable considering that the amount of H incorporated in the films at 1100°C is also expected to be weakly dependent on time on the time scale of Fig. 2. This is because the H diffusion length for this time scale, as estimated from the effective H diffusivity [35] in SiO_2 , is much larger than the film thickness of $2 \mu\text{m}$. The enhancement of the PL upon H incorporation has also been observed in the $\text{Si}_y\text{O}_{1-y}$ films obtained by the Si ion implantation in SiO_2 and annealed in the gas formed and has been attributed to the passivation of the nonradiative recombination centers, such as Si-dbs, by the H atoms [26]–[31].

The enhancement of the PL intensity in the samples annealed in ($\text{Ar} + 5\% \text{H}_2$) is also observed [18] for the $\text{Si}_y\text{O}_{1-y}$ films with different values of y . The amount of the enhancement and its spectral dependence are quantitatively different for different compositions. Fig. 3 shows the enhancement ratio (ER), defined as the ratio between the PL intensities from a sample annealed in ($\text{Ar} + 5\% \text{H}_2$) and that from the identical samples annealed in pure Ar under otherwise identical annealing conditions (1100°C), for two different values of y and three different annealing times.

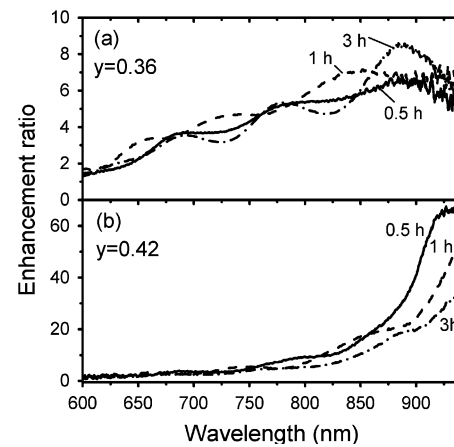


Fig. 3. Enhancement ratio [the ratio between the PL intensity from a sample annealed in ($\text{Ar} + 5\% \text{H}_2$) and that from an identical sample annealed in the pure Ar under otherwise identical annealing conditions] as a function of the PL wavelength for the $\text{Si}_y\text{O}_{1-y}$ films. (a) $y = 0.36$. (b) $y = 0.42$. The annealing temperature was 1100°C and the annealing durations were 0.5 h (solid line), 1 h (dashed line), and 3 h (dash-dotted line). The modulation of the lines is likely due to the interference effects.

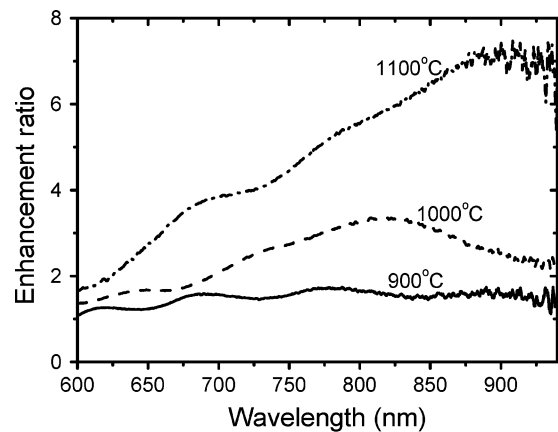


Fig. 4. Enhancement ratio (as defined in Fig. 3) as a function of the PL wavelength for $\text{Si}_y\text{O}_{1-y}$ films with $y = 0.36$ at annealing temperatures of 900°C (solid line), 1000°C (dashed line), and 1100°C (dash-dotted line). The annealing duration was 2 h.

Fig. 3(a) and (b) shows that the ER increases with the increasing wavelength. This result reflects the fact that, as reported in a recent publication [33], the replacement of Ar by ($\text{Ar} + 5\% \text{H}_2$) in the annealing preferentially promotes emissions at longer wavelengths. In addition, the ER for the sample with larger Si content increases faster with the increasing wavelength, reaching significantly larger ER values in the long wavelength range as compared to $y = 0.36$. It is important to note, however, that the overall PL intensity for the $y = 0.42$ sample is always significantly lower than that for the $y = 0.36$ sample [33]. This is consistent with what is expected from the QC, since for larger y , larger Si-ncs are formed, which should lead to a reduced smearing out of the excitonic wavefunctions and, therefore, reduced bandgap transition probabilities.

Similar to Fig. 2, Fig. 3 also indicates that the annealing time does not have a significant effect on the ER, except for the longer wavelengths in the $y = 0.42$ sample. In this case, the ERs decrease slightly with the increasing annealing time.

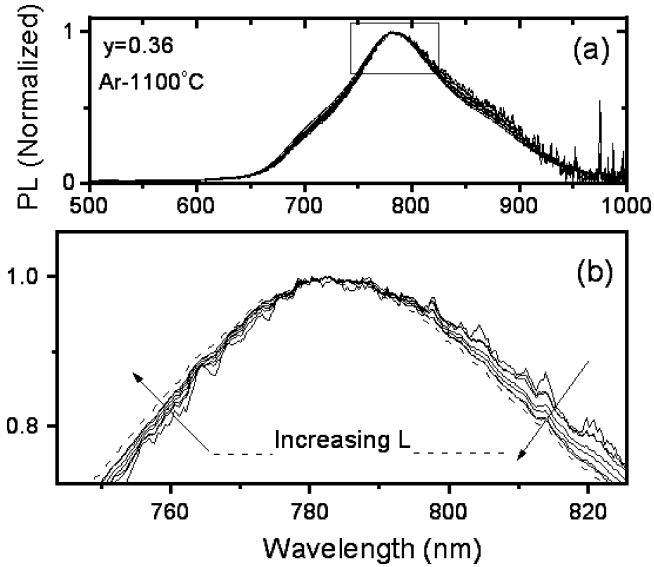


Fig. 5. (a) Normalized PL spectra as measured for different pump laser power (L) for a $\text{Si}_y\text{O}_{1-y}$ film with $y = 0.36$ annealed at 1100°C for 3 h in pure Ar. (b) Close-up view of the *inset* square region shown in (a). The spectral variation trends with increasing L are indicated by *arrows*. The *dashed line* represents the PL spectrum as measured with the full pump laser power.

Fig. 4 shows the spectral dependence of the ER for the sample with $y = 0.36$ for various annealing temperatures. ER becomes a more steeply increasing function of the wavelength as T increases. This indicates that the combined process of the Si-nc formation by the Si precipitation and passivation by H of the nonradiative recombination centers is significantly improved as T increases. Also apparent from Fig. 4 is that the preferential activation of the long-wavelength emissions induced by the annealing in (Ar + 5% H_2) occurs most significantly when T reaches the value of 1100°C .

B. Dependence on the Pump Laser Power

In order to gain some more insight in the PL mechanisms, the PL for samples annealed in the pure Ar and in (Ar + 5% H_2) was measured as a function of the pump power. The normalized spectra obtained for the sample with $y = 0.36$ are shown in Figs. 5 and 6. Two main features can be noticed in these figures. First, the PL spectral shape changes only slightly (but noticeably) with increasing L for the sample annealed in Ar (Fig. 5) and more significantly for the sample annealed in (Ar + 5% H_2) (Fig. 6). Second, in both the cases, these changes are characterized by a skew of the spectra to the blue as L increases. These results indicate that the PL decay rate depends on the wavelength in a way that is qualitatively similar, but quantitatively different, for the samples annealed in (Ar + 5% H_2) as compared to those annealed in Ar. As shown in the next section, the overall behavior is consistent with a PL decay model for the Si-ncs embedded in SiO_2 .

C. H-Bonding in As-Grown and Annealed Samples

The full FTIR spectra for the samples considered here were presented previously and the modes associated with the Si-O

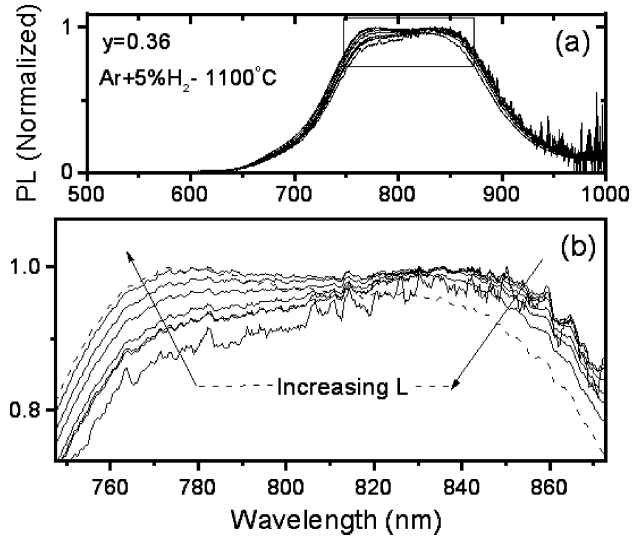


Fig. 6. (a) Normalized PL spectra as measured for different pump laser power (L) for a $\text{Si}_y\text{O}_{1-y}$ film with $y = 0.36$ annealed at 1100°C for 3 h in (Ar + 5% H_2). (b) Close-up view of the *inset* square region shown in (a). The spectral variation trends with increasing L are indicated by *arrows*. The *dashed line* represents the PL spectrum as measured with the full pump laser power. The apparent double peak structure is an artifact due to a multiple interference-related dip on the peak maximum regions.

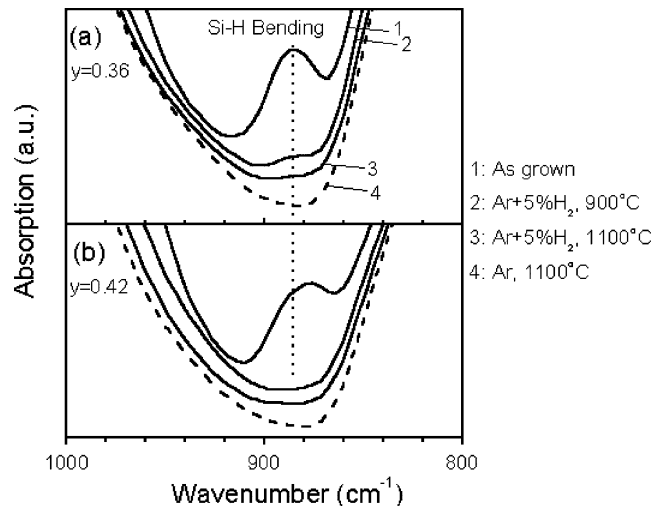


Fig. 7. FTIR absorption spectra in the region of the Si-H bending mode for the $\text{Si}_y\text{O}_{1-y}$ films. (a) $y = 0.36$. (b) $y = 0.42$. The general shape of the spectra is dominated by a strong minimum associated with the interference fringes due to the multiple reflections of the probe beam in the films. From *top to bottom*: (1) As-grown samples. (2) Annealed at 900°C in (Ar + 5% H_2). (3) Annealed at 1100°C in (Ar + 5% H_2). (4) Annealed at 1100°C in Ar. The annealing duration was 2 h. Note the traces of the Si-H bending mode detected as flat-bottomed minima in the data for the samples annealed in (Ar + 5% H_2).

bonds in the oxide were thoroughly discussed [18]. No peaks due to the OH groups were detected, indicating that the bonded H incorporates mainly as Si-H bonds. A close up around the Si-H bending mode is shown in Fig. 7 for samples with $y = 0.36$ and 0.42. It can be seen that the as-grown $y = 0.36$ film clearly presents the Si-H bending peak at 882 cm^{-1} , which is also observed, slightly shifted to a lower wavenumber, in the sample with $y = 0.42$. The shift of the peak to a lower wavenumber

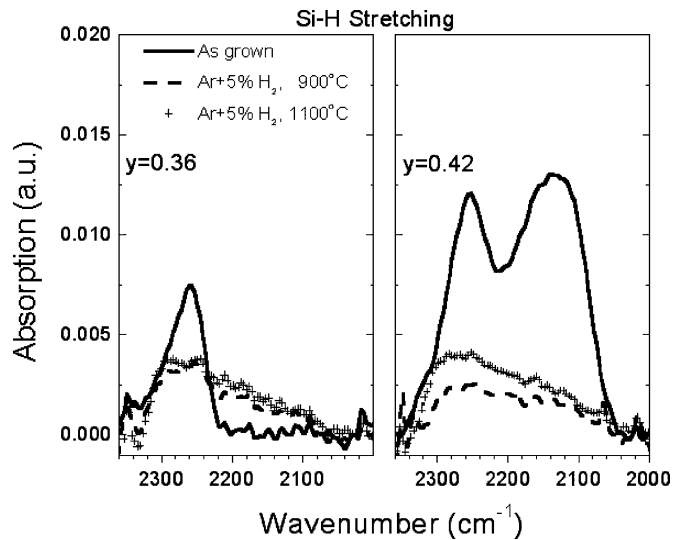


Fig. 8. FTIR absorption spectra in the region of the Si–H stretching mode for the $\text{Si}_y\text{O}_{1-y}$ films. (Left) $y = 0.36$. (Right) $y = 0.42$. The spectra were background-corrected for the interference effects due to the multiple reflections. As-grown (Solid lines). Annealed at 900°C in (Ar + 5% H_2) (dashed lines). Annealed at 1100°C in (Ar + 5% H_2) (+). The annealing duration was 2 h.

with increasing y has been observed before and is due to the increasing replacement of O by the less electronegative Si in $\text{Si-O}_n\text{Si}_{1-n}$ ($4 \geq n \geq 0$) tetrahedral units [36]. The peak intensity is reduced to less than the present FTIR detection limit when the films are annealed under Ar at 1100°C . The ERDA measurements show that the H concentration is reduced to values lower than the detection limit of 0.1 at.% due to the H exodiffusion, as found previously in similar samples [37]. Hence, the trace observed for the samples annealed in (Ar + 5% H_2) corresponds to the H incorporated during annealing to a concentration probably close to the solubility limit of H in the $\text{Si}_y\text{O}_{1-y}$ films.

Unfortunately, this H incorporation, although barely detectable by the FTIR, is still less than our present ERDA detection limit of 0.1 at.%. Fig. 8 shows the FTIR absorption spectra in the Si–H stretching region for both $y = 0.36$ and 0.42 . For the as-grown film with the low Si content, a single peak is observed at about 2260 cm^{-1} , characteristic of the nearly stoichiometric (SiO_2) materials [36]. For $y = 0.42$, an additional peak close to 2130 cm^{-1} is also present. This behavior is normally observed in the $\text{Si}_y\text{O}_{1-y}$ films with the intermediate values of y (i.e., y not too close to either $1/3$ or 1), and it can be attributed to the combined induction effects due to the nearest and remote neighbors [38] of the Si atom to which the H is attached. As can be seen in Fig. 8, after annealing, the peak intensities are strongly reduced due to the reduction of the H content in the films. The differences in the shape and intensity observed between the spectra for the as-grown samples in Fig. 8(a) and (b) are nearly lost upon annealing. This is because phase separation occurs [13], [14] and, in both the cases, an amorphous SiO_2 matrix is formed whose bonded H gives the largest contribution to the peak associated with the stretching Si–H mode at about 2260 cm^{-1} . Note, however, that the vibrations of the H atoms bonded to the Si atoms at the Si-nc interfaces are likely to contribute to the absorption less than 2200 cm^{-1} as the induction

effects due to the backbonded Si atoms from the Si-nc core act in a way to reduce the mode frequency [38].

IV. DISCUSSION

Previous studies of the structure of the $\text{Si}_y\text{O}_{1-y}$ films annealed under the inert and H_2 -containing atmospheres have shown that the inclusion of H_2 does not significantly influence the Si-nc mean density or size [33], [39]. This observation is consistent with the recent theoretical predictions [23] of the negligible size modifications in the Si-ncs upon H passivation. Diffraction measurements [18] of the Si(1 1 1) Bragg peak in samples similar to those considered here have estimated a mean Si-nc diameter of $\sim 5.2\text{ nm}$ for $y = 0.42$ and $< 2\text{ nm}$ for $y = 0.36$ for the samples annealed either in Ar or in (Ar + 5% H_2).

The present ERDA results show that the concentration of both the bonded and the nonbonded H in materials annealed at temperatures above 1000°C is below the detection limit of 0.1 at.%. No signs of Si–H bonds are detected by the FTIR in the samples annealed at the same temperatures in pure Ar (see, for instance, Fig. 7 and also [18]). In the films annealed in (Ar + 5% H_2), however, traces of Si–H bonds are detected, mainly through the Si–H stretching modes (Fig. 8). From the FTIR traces, we estimate the H concentration of the order of a few times 10^{-2} at.%. This value should be close to the chemical solubility of H_2 in the Si-nc/ SiO_2 composite lattice at the annealing temperature or at a certain (somewhat lower) effective temperature determined by the cooling rate down to room temperature at the end of the annealing run. Hence, it can be concluded that the Si–H traces detected by the FTIR in (Ar + 5% H_2) annealed materials are due to the H incorporated in the annealing process, and not due to the thin film growth. These Si–H bonds are primarily due to the Si atoms backbonded to three O atoms in the SiO_2 matrix, which contribute to the Si–H stretching peak at about 2250 cm^{-1} . Nevertheless, signs of the H atoms bonded to the Si atoms backbonded by one or more nearest neighbors of Si are also found as contributions to the absorption at wavenumbers below 2200 cm^{-1} in Fig. 8. Since, at 1100°C , the SiO_2/Si phase separation process is nearly completed [13], [14], it is very likely that some of these contributions are due to the H at the Si-nc/ SiO_2 interface regions, which are expectedly highly disordered and rich in dbs.

Concomitant with these H-bonding changes upon annealing in either Ar or (Ar + 5% H_2), Si-ncs are formed and the PL intensity in the visible emerges above the detection limit, increasing significantly with the increasing annealing temperature (Fig. 1) and time (Fig. 2). This increase is larger when the samples are annealed in (Ar + 5% H_2). Since the same annealing procedures have been shown to lead to the phase separation and Si-nc formation [18], it is very likely that the observed PL is associated with the excitation of the Si-ncs. Although we lack rigorous proof at this stage, the bulk of the presently available data indicates that the PL has its origin linked to QC in the Si-ncs. First, we observe a redshift of the PL peak with the increasing Si-nc size (i.e., with the increasing y and T). Second, the intensity of the PL is negligible for the stoichiometric materials, it is the maximum for

$y = 0.36$, and decreases with the increasing y , as expected from a diminishing QC effect for the increasing Si-nc size [12], [18].

Regarding the effects of H, it is interesting that H itself, without Si-nc formation, does not lead to any luminescence, as could be expected if siloxene [25] or other luminescent Si-H complexes [40] were formed. This is the case of the as-grown $\text{Si}_y\text{O}_{1-y}$ films, which contain several atomic percent of the bonded H that are incorporated from the SiH_4 precursor in the PECVD process. In contrast, its incorporation by the H_2 diffusion from the (Ar + 5% H_2) gas during the annealing process—while Si-ncs are formed—leads to the strong enhancement of the PL. This fact is consistent with the hypothesis that the main role of the H is to passivate the nonradiative recombination centers, very likely Si dbs in the Si-nc/ SiO_2 interface regions. In view of the fact that the behavior of the PL intensity as a function of the annealing parameters, Si content, and pump power is very similar for the samples annealed in either (Ar + 5% H_2) or Ar, it is also very unlikely that the H introduces new luminescence centers other than Si-ncs, such as siloxene, during the annealing.

In addition, the enhancement of the PL induced by the H occurs, for both the Si concentrations studied here, at wavelengths longer than the peak wavelength that is observed when the samples are annealed in pure Ar (see Fig. 3 and [33]). This clearly supports the interpretation that H passivates preferentially dbs close to the disordered Si-ncs where radiative transitions between disorder-induced bandgap states occurs [18], [33]. That is to say, as the Si content increases, larger Si-ncs are formed with the corresponding narrower Si-nc bandgaps, which result in a red-shift of the PL peak with the increasing y . The H-enhanced PL contributions, in turn, also shift to longer wavelengths with the increasing y (Fig. 3) because the disorder-induced bandgap states tend to become closer to each other as the Si-nc bandgaps become narrower.

We now turn our attention to the power dependence of the PL spectra. As seen in Figs. 5 and 6, the relative contributions at long wavelengths decrease while the contributions at short wavelengths increase as the laser power is increased. This effect is observed for the samples annealed in either Ar or (Ar + 5% H_2), although it is more noticeable for the latter, and it can be characterized by plotting the PL intensity at different wavelengths as a function of the laser power (Fig. 9). It can be seen that the data points can be well represented by a power law $\text{PL} = A(L)^b$, where A is a proportionality constant and b is always very close to unity, but depends slightly on the wavelength and the annealing ambient.

For the light emission from the isolated quantum dots, a linear dependence ($b = 1$) is expected at low pump power [41]–[43]. For L high enough, when virtually all the dots are already excited, a saturation regime might be approached where b will become gradually lesser than unity [42], [43]. Hence, one would expect the saturation regime to be achieved earlier (i.e., at lower values of L), when the number of the quantum dots is relatively small or the decay time is relatively long.

Returning to Fig. 9, we observe that b is consistently lower for the samples annealed in Ar than for those annealed in (Ar +

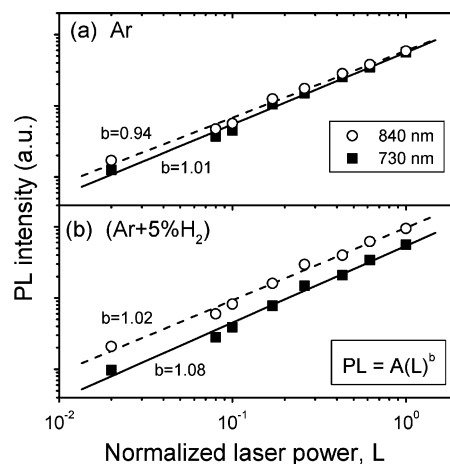


Fig. 9. The PL intensity (PL) as a function of the laser power (L) for the $\text{Si}_y\text{O}_{1-y}$ films with $y = 0.36$ annealed at 1100°C for 3 h, and measured at two different wavelengths: 840 nm (open circles) and 730 nm (squares). (a) Annealing in pure Ar. (b) Annealing in (Ar + 5% H_2). L is normalized to its maximum value obtained for the full pump laser power. The solid and dashed lines are least-squares fits of the equation $\text{PL} = A(L)^b$ to the corresponding experimental data. The values of b obtained from the fits are indicated; the present uncertainty in their determination is $\Delta b \approx 0.04$.

5% H_2) for each of both the wavelengths considered. This is in general agreement with what is expected from the arguments given above; namely, in the unpassivated (Ar-annealed) sample, the number of the light-emitting Si-ncs is significantly smaller than in the passivated [(Ar + 5% H_2)-annealed] sample, leading to the slightly lower b . Migration of the electrons and holes across the barrier material between the neighboring dots have been invoked to explain a blueshift of the PL peak observed with the increasing laser power [44] in the Si-nc/ SiO_2 composites. In our case, both Figs. 5 and 6 do not show a clear blueshift of the peak; however, they do reveal a skew of the PL spectra to the blue for both the Ar and (Ar + 5% H_2) annealing with the increasing L . The laser power induced blueshift can be explained [44] by a PL decay model that considers the tunneling of electrons from the Si-nc to the surrounding SiO_2 matrix where they recombine nonradiatively [45]. The tunneling probability of the photoexcited electron in the Si-nc increases when its energy increases, which leads to a corresponding decrease in the decay lifetime. Since a smaller electron energy corresponds to the light emission at longer wavelengths, longer decay times are, indeed, expected for the PL contributions at longer wavelengths. This is in agreement with what is deduced from the power dependence data of Figs. 5, 6, and 9, which indicate a weaker dependence of the PL on L (i.e., an earlier approach to a sublinear regime) at longer wavelengths. Alternative possible models to explain the blueshift of the PL spectra from the Si-ncs have also been given [43]. Clearly, further studies of the PL are needed to give a detailed description of the recombination mechanisms.

Nevertheless, the present power dependence data for the $\text{Si}_y\text{O}_{1-y}$ samples annealed in either Ar or (Ar + 5% H_2) are in qualitative agreement with the previous results and decay models proposed for the PL from the Si-nc quantum dots embedded in SiO_2 . The fact that the decay time differences are more noticeable in the (Ar + 5% H_2) case (compare Fig. 6 with

Fig. 5) is probably related to the fact that the PL peak, in this case, is wider, hence spanning a wider range of the electron energies. The widening of the PL peak for the (Ar + 5% H₂) annealed sample with respect to that for the film annealed in the pure Ar reflects a widening of the bandgap energy distribution of the light-emitting Si-ncs. Since this widening is accompanied by a skew of the whole PL spectrum to the red, it seems that the small-bandgap Si-ncs are preferentially activated by the H passivation in the (Ar + 5% H₂) annealing step. The small-bandgap Si-ncs could result from either large Si-nc sizes [31] or from disorder-induced bandgap narrowing [33]. Possible models to explain why such small bandgap Si-ncs would be preferentially deactivated by the dbs in the unpassivated materials (and preferentially passivated by H under H₂ treatments) have been given in the literature [31], [33].

V. CONCLUSION

The PL of the hydrogenated and unhydrogenated Si-nc/SiO₂ composites obtained from the ECR-PECVD Si_yO_{1-y} thin films was studied for two different Si contents above the stoichiometric value as a function of the annealing parameters and the laser pump power. The H was incorporated into the samples by annealing them in (Ar + 5% H₂) and the H bonding was studied by the FTIR. The dependence of the PL spectra on y , T , and laser power indicates that the light emission in these materials is linked to the QC in Si-ncs. Further work is needed to confirm the exact mechanism of the light emission and the details of the recombination process. H incorporates as Si-H bonds and leads to a strong increase of the PL intensity and to a skew of the PL spectrum to the red. This behavior, and the dependence of the PL spectra on the laser power, indicate that the H passivates the nonradiative recombination centers, most probably Si dbs at the Si-nc/SiO₂ regions. This process results in the activation of many Si-ncs that incorporate into the ensemble of the light-emitting Si-ncs in the samples, increasing their total number by several hundred percent and skewing the bandgap energy distribution to the lower energy side. These results provide new insight in the mechanisms of the H passivation of the Si-nanostructures based on the substoichiometric Si_yO_{1-y} films fabricated by the PECVD, and are expected to be relevant for the optimization of the light-emission efficiency and tunability in future developments of the Si-light sources.

ACKNOWLEDGMENT

The authors gratefully acknowledge Prof. W. Lennard for help with the ERDA measurements, E. A. Irving for help in the sample growth, and M. Flynn and T. Roschuk for fruitful discussions.

REFERENCES

- [1] L. Pavesi and D. J. Lockwood, Eds., *Silicon Photonics*. Berlin, Germany: Springer-Verlag, 2004.
- [2] M. Salib, L. Liao, R. Jones, M. Morse, A. Liu, D. Samara-Rubio, A. Alduino, and M. Paniccia. (2004, May) Silicon photonics. *Intel Technol. J.* [Online] 8(2), pp. 143–160. Available: <http://developer.intel.com/technology/itj/2004/volume08issue02/>
- [3] R. J. Walters, G. I. Bourianoff, and H. A. Atwater, "Field-effect electroluminescence in silicon nanocrystals," *Nat. Mater.*, vol. 4, pp. 143–146, Feb. 2005.
- [4] L. Pavesi, L. Dal Negro, C. Mazzoleni, G. Franzo, and F. Priolo, "Optical gain in silicon nanocrystals," *Nature*, vol. 408, pp. 440–444, Nov. 2000.
- [5] P. M. Fauchet, "Monolithic silicon light sources," *Topics Appl. Phys.*, vol. 94, pp. 177–198, 2004.
- [6] H. S. Rong, A. S. Liu, R. Jones, O. Cohen, D. Hak, R. Nicolaescu, A. Fang, and M. Paniccia, "An all silicon Raman laser," *Nature*, vol. 433, pp. 292–294, Jan. 2005.
- [7] L. T. Canham, "Silicon quantum wire array fabrication by electrochemical and chemical dissolution of wafers," *Appl. Phys. Lett.*, vol. 57, pp. 1046–1048, Sep. 1990.
- [8] L. Pavesi, "Influence of dispersive exciton motion on the recombination dynamics in porous silicon," *J. Appl. Phys.*, vol. 80, pp. 216–225, Jul. 1996.
- [9] M. A. Tischler, R. T. Collins, J. H. Stathis, and J. C. Tsang, "Luminescence degradation in porous silicon," *Appl. Phys. Lett.*, vol. 60, pp. 639–641, Feb. 1992.
- [10] T. Shimizu-Iwayama, Y. Terao, A. Kamiya, M. Takeda, S. Nakao, and K. Saitoh, "Visible photoluminescence from silicon nanocrystals formed in silicon dioxide by ion implantation and thermal processing," *Thin Solid Films*, vol. 276, pp. 104–107, Apr. 1996.
- [11] F. Iacona, G. Franzo, and C. Spinella, "Correlation between luminescence and structural properties of Si nanocrystals," *J. Appl. Phys.*, vol. 87, pp. 1295–1303, Feb. 2000.
- [12] T. Roschuk, J. Wojcik, E. A. Irving, M. Flynn, and P. Mascher, "Silicon nanocrystal formation in silicon rich silicon oxide thin films," in *Proc. SPIE*, vol. 5577, pp. 450–458, 2004.
- [13] D. Comedi, O. H. Y. Zalloum, E. A. Irving, J. Wojcik, T. Roschuk, M. J. Flynn, and P. Mascher, "Si/SiO₂ phase separation during high-temperature annealing of a-Si_yO_{1-y} films studied by grazing angle X-ray diffraction," unpublished.
- [14] —, "X-ray diffraction study of crystalline Si nanocluster formation in annealed silicon-rich silicon oxides," *J. Appl. Phys.*, vol. 99, pp. 023518-1–023518-8, Jan. 2006.
- [15] F. Iacona, C. Bongiorno, C. Spinella, S. Boninelli, and F. Priolo, "Formation and evolution of luminescent Si nanoclusters produced by thermal annealing of SiO_x films," *J. Appl. Phys.*, vol. 95, pp. 3723–3732, Apr. 2004.
- [16] C. Bonafos, B. Colombeau, A. Altibelli, M. Carrada, G. B. Assayag, B. Garrido, M. Lopez, A. Perez-Rodriguez, J. R. Morante, and A. Claverie, "Kinetic study of group IV nanoparticles ion beam synthesized in SiO₂," *Nucl. Instrum. Methods B*, vol. 178, pp. 17–24, May 2001.
- [17] T. Roschuk, J. Wojcik, D. Comedi, M. J. Flynn, E. A. Irving, O. H. Y. Zalloum, and P. Mascher, "Optical properties of nanostructures based on silicon rich silicon oxide (RSO) thin films," in *Proc. Electrochem. Soc.*, vol. 2005-01, R. E. Sah, M. J. Deen, J. Yota, J. F. Zhang, and Y. Kamakura, Eds., 2005, pp. 136–147.
- [18] D. Comedi, O. H. Y. Zalloum, E. A. Irving, J. Wojcik, and P. Mascher, "H-induced effects in luminescent silicon nanostructures obtained from PECVD grown Si_yO_{1-y}:H ($y > 1/3$) thin films annealed in (Ar + 5% H₂)," *J. Vac. Sci. Technol. A.*, vol. 24, pp. 817–820, May 2006.
- [19] N. Daldosso, M. Luppi, S. Ossini, E. Degoli, R. Magri, G. Dalba, P. Fornasini, R. Grisenti, F. Rocca, L. Pavesi, S. Boninelli, F. Priolo, C. Spinella, and F. Iacona, "Role of the interface region on the optoelectronic properties of silicon nanocrystals embedded in SiO₂," *Phys. Rev. B, Condens. Matter*, vol. 68, pp. 085327-1–085327-8, Aug. 2003.
- [20] C. Temon, C. Dufour, F. Gourbilleau, and R. Rizk, "Roles of interfaces in nanostructured silicon luminescence," *Eur. Phys. J. B*, vol. 41, pp. 325–332, Oct. 2004.
- [21] A. Puzder, A. J. Williamson, J. C. Grossman, and G. Galli, "Surface chemistry of silicon nanoclusters," *Phys. Rev. Lett.*, vol. 88, pp. 097401-1–097401-4, Mar. 2002.
- [22] M. Lannoo, C. Delerue, and G. Allan, "Theory of radiative and nonradiative transitions for semiconductor nanocrystals," *J. Lumin.*, vol. 70, pp. 170–184, 1996.
- [23] D. K. Yu, R. Q. Zhang, and S. T. Lee, "Structural properties of hydrogenated silicon nanocrystals and nanoclusters," *J. Appl. Phys.*, vol. 92, pp. 7453–7458, Dec. 2002.
- [24] M. Nishida, "Effect of alloying of Si with hydrogen on the electronic structure of spherical Si nanocrystals," *Phys. Rev. B, Condens. Matter*, vol. 70, pp. 113303-1–113303-4, Sep. 2004.

- [25] H. D. Fuchs, M. Stutzmann, M. S. Brandt, M. Rosenbauer, J. Weber, A. Breitschwerdt, P. Deak, and M. Cardona, "Porous silicon and siloxene: Vibrational and structural properties," *Phys. Rev. B, Condens. Matter*, vol. 48, pp. 8172–8189, Sep. 1993.
- [26] T. Komoda, J. P. Kelly, R. M. Gwilliam, P. L. F. Hemment, and B. J. Sealy, "Effect of the ambient on the intensity of the visible photoluminescence from Si microcrystallites in a SiO₂ matrix formed by ion implantation," *Nucl. Instrum. Methods B*, vol. 112, pp. 219–222, May 1996.
- [27] M. Lopez, B. Garrido, C. Garcia, P. Pellegrino, A. Perez-Rodriguez, J. R. Morante, C. Bonafos, M. Carrada, and A. Claverie, "Elucidation of the surface passivation role on the photoluminescence emission yield of silicon nanocrystals embedded in SiO₂," *Appl. Phys. Lett.*, vol. 80, pp. 1637–1639, Mar. 2002.
- [28] A. R. Wilkinson and R. G. Elliman, "Passivation of Si nanocrystals in SiO₂: Atomic versus molecular hydrogen," *Appl. Phys. Lett.*, vol. 83, pp. 5512–5514, Dec. 2003.
- [29] S. P. Withrow, C. W. White, A. Meldrum, J. D. Budai, D. M. Hembree, Jr., and J. C. Barbour, "Effects of hydrogen in the annealing environment on photoluminescence from Si nanoparticles in SiO₂," *J. Appl. Phys.*, vol. 86, pp. 396–401, Jul. 1999.
- [30] S. Cheylan and R. G. Elliman, "Effect of hydrogen on the photoluminescence of Si nanocrystals embedded in a SiO₂ matrix," *Appl. Phys. Lett.*, vol. 78, pp. 1225–1227, Feb. 2001.
- [31] —, "Effect of particle size on the photoluminescence from hydrogen passivated Si nanocrystals in SiO₂," *Appl. Phys. Lett.*, vol. 78, pp. 1912–1914, Mar. 2001.
- [32] M. Boudreau, M. Boumerzoug, P. Mascher, and P. E. Jessop, "Electron-cyclotron-resonance chemical vapor deposition of silicon oxynitrides using tris(dimethylamino)silane," *Appl. Phys. Lett.*, vol. 63, pp. 3014–3016, Nov. 1993.
- [33] D. Comedi, O. H. Y. Zalloum, and P. Mascher, "H-sensitive radiative recombination path in Si-nanoclusters embedded in SiO₂," *Appl. Phys. Lett.*, vol. 87, pp. 213110-1–213110-3, Nov. 2005.
- [34] S. M. Orbons, M. G. Spooner, and R. G. Elliman, "Effect of material structure on photoluminescence spectra from silicon nanocrystals," *J. Appl. Phys.*, vol. 96, pp. 4650–4652, Oct. 2004.
- [35] V. Lou, R. Sato, and M. Tomozawa, "Hydrogen diffusion in fused silica at high temperatures," *J. Non-Cryst. Solids*, vol. 315, pp. 13–19, Jan. 2003.
- [36] A. Sassella, A. Borghesi, F. Corni, A. Monelli, G. Ottaviani, R. Tonini, B. Pivac, M. Bacchetta, and L. Zanotti, "Infrared study of Si-rich silicon oxide films deposited by plasma-enhanced chemical vapor deposition," *J. Vac. Sci. Technol. A*, vol. 15, pp. 377–389, Mar./Apr. 1997.
- [37] T. Roschuk, J. Wojcik, and P. Mascher, "Optical and compositional analysis of annealed SiO_x thin films deposited by electron cyclotron resonance plasma enhanced chemical vapor deposition," presented at the Soc. Vacuum Coaters (SVC) 47th Annual Tech. Conf., Dallas, TX, 2004.
- [38] G. Lucovsky, "Atomic structure and thermal stability of silicon suboxides in bulk thin films and in transition regions at Si–SiO₂ interfaces," *J. Non-Cryst. Solids*, vol. 227–230, pp. 1–14, May 1998.
- [39] Y. Q. Wang, R. Smirani, and G. G. Ross, "Effect of hydrogen passivation on the microstructure of silicon nanocrystals in SiO₂," *Physica E*, vol. 23, pp. 97–101, Jun. 2004.
- [40] C. Tsai, K. H. Li, D. S. Kinosky, R. Z. Qian, T. C. Hsu, J. T. Irby, S. K. Banerjee, A. F. Tasch, J. C. Campbell, B. K. Hance, and J. M. White, "Correlation between silicon hydride species and the photoluminescence intensity of porous silicon," *Appl. Phys. Lett.*, vol. 60, pp. 1700–1702, Apr. 1992.
- [41] E. C. Le Ru, J. Fack, and R. Murray, "Temperature and excitation density dependence of the photoluminescence from annealed InAs/GaAs quantum dots," *Phys. Rev. B, Condens. Matter*, vol. 67, pp. 245318-1–245318-12, Jun. 2003.
- [42] V. Vinciguerra, G. Franzo, F. Priolo, F. Iacona, and C. Spinella, "Quantum confinement and recombination dynamics in silicon nanocrystals embedded in Si/SiO₂ superlattices," *J. Appl. Phys.*, vol. 87, pp. 8165–8173, Jun. 2000.
- [43] D. Kovalev, H. Heckler, G. Polisski, and F. Koch, "Optical properties of Si nanocrystals," *Phys. Status Solidi B*, vol. 215, pp. 871–932, Oct. 1999.
- [44] A. Hryciw, A. Meldrum, K. S. Buchanan, and C. W. White, "Effects of particle size and excitation spectrum on the photoluminescence of silicon nanocrystals formed by ion implantation," *Nucl. Instrum. Methods B*, vol. 222, pp. 469–476, Aug. 2004.
- [45] J. C. Vial, A. Bsiesty, F. Gaspard, R. Herino, M. Ligeon, F. Muller, R. Romestain, and R. M. Macfarlane, "Mechanisms of visible-light emission from electrooxidized porous silicon," *Phys. Rev. B, Condens. Matter*, vol. 45, pp. 14171–14176, Jun. 1992.

David Comedi was born in Tucuman, Argentina, in 1961. He received the B.A., M.Sc., and Ph.D. degrees from Technion – Israel Institute of Technology, Haifa, Israel, in 1983, 1986, and 1990, respectively, all in physics.

From 1990 to 1993, he was a Postdoctoral Fellow at the Centre for Electrophotonic Materials and Devices, McMaster University, Hamilton, ON, Canada. In 1993, he was a Visiting Scientist at the Institute of Physics "Gleb Wataghin," State University of Campinas (Unicamp), Brazil, where he became an Associate Researcher of physics in 1994, an Assistant Professor in 1997, and an Associate Professor in 1999. He was a Visiting Scientist at the Centre for Emerging Device Technologies (CEDT), McMaster University, where he was engaged in the physics of the luminescent Si-based nanostructures, Si nanocluster formation, and Si–SiO₂ phase separation phenomena in Si-rich silicon oxides, and helped to promote scientific collaborations between the CEDT and South America. He is currently with the Universidad Nacional de Tucumán, Tucumán, Argentina. He is the author or coauthor of 44 articles published in refereed journals, 11 in refereed conference proceedings, and a review encyclopedic article on the properties of amorphous semiconductors. His current research interests include the fields of ion-solid interactions, ion-beam assisted thin film deposition, doping, defect spectroscopy, and electronic structure of non-crystalline semiconductors, luminescence, and the structure of semiconductor alloys and nanostructured composites.

Dr. Comedi is the recipient of the title "Livre-Docencia" for the year 2001 awarded by Unicamp for his studies on the electronic structure and electronic, optical, and magnetic properties of condensed matter. He has been a reviewer for various scientific journals, and was a member of the Editorial Board of the Brazilian literary magazine *Humanus* between 2000 and 2003.

Othman H. Y. Zalloum received the B.Eng. (honors), M.Sc. (experimental physics), and Ph.D. (experimental physics) degrees from the National University of Ireland, Dublin, Ireland, in 1990, 1991, and 1994, respectively. He also received the National Certificate in Electronic Engineering with credit from Waterford Institute of Technology, Waterford, Ireland, in 1986.

He was an Assistant Professor of Physics at Al-Zaytoonah University of Jordan, Amman, Jordan for the period 1995–1997. From 1997 to 1998, he was an Assistant Professor of Physics at Al-Zarka University, Zarka, Jordan. From 1998 to 2002, he was an Assistant Professor of Physics with a cross appointment to the Faculty of Engineering at Palestine Polytechnic University, Hebron, Palestine. During 2003, he was a Postdoctoral Fellow and a Research Associate in Ophthalmic Optics at the Wilmer Eye Institute of The Johns Hopkins University School of Medicine, Baltimore, MD. In 2004, he joined McMaster University, Hamilton, ON, Canada. His current interests include optical and electrical characterization techniques for thin films and optoelectronic devices.

Dr. Zalloum is a Chartered Physicist and a member of the Institute of Physics (United Kingdom) and was elected a Chartered Engineer by the British Engineering Council in 1997. He is also a member of the European Optical Society. He was the Executive Vice President of the Johns Hopkins Postdoctoral Association in 2003 and is the recipient of the Canon Scholarship Award and a Certificate of Distinction from Cantec in association with the Dublin Institute of Technology for outstanding project work at University College, Dublin, and the award of the Institution of Mechanical Engineers (United Kingdom) for outstanding project work at University College, Dublin, both in 1990.

Jacek Wojcik was born in Wrocław, Poland, in 1970. He received the Master's degree in physics and the Ph.D. degree in applied physics from Wrocław University of Technology, Wrocław, in 1994 and 1999, respectively.

He joined McMaster University, Hamilton, ON, Canada, as a Postdoctoral Fellow in 2000, where he became a Research Scientist in the Department of Engineering Physics in 2002, and where he is currently engaged in thin films deposition laboratory including ICP-CVD, ECR-PECVD, RF-sputtering, E-beam. His current research interests include thin film materials such as SiO_xN_y and Si-nc (silicon nanocrystals) materials imbedded in SRSO (silicon rich silicon oxides) and ellipsometric determination of thin film properties. He is the author or coauthor of more than 40 scientific papers published in national and international physics journals.



Peter Mascher received the Ph.D. degree in engineering physics from the Technical University Graz, Styria, Austria, in 1984.

He was a Postdoctoral Fellow and a Research Associate at the University of Winnipeg. In 1989, he joined McMaster University, Hamilton, ON, Canada, where he became a Professional Engineer and a Professor in the Department of Engineering Physics, and he was the Chair of the department from 1995 to 2001. Currently, he is the Associate Dean (Research and External Relations) of the Faculty of Engineering. He

leads active research groups involved in the fabrication and characterization of thin films for optoelectronic applications and defects in semiconductors by positron annihilation spectroscopy. He is the author or coauthor of more than 140 publications in refereed journals and conference proceedings and has presented many invited lectures at international conferences and workshops. He is a member of McMaster's Brockhouse Institute for Materials Research and the Centre for Emerging Device Technologies. In 2001, he was the William Sinclair Chair in Optoelectronics. Since 2003, he has been the Program Director of the Ontario Photonics Consortium, McMaster University-led multi-university initiative co-funded by the Ontario Research and Development Challenge Fund and industrial partners.

Dr. Mascher is also a member of various international physics and materials research societies.